Available online at www.sciencedirect.com
ScienceDirect
Proceedings of the Combustion Institute 32 (2009) 377–385
Proceedings of the Combustion Institute
www.elsevier.com/locate/proci

Fuel dependence of benzene pathways

Hongzhi R. Zhang [a,*], Eric G. Eddings [a], Adel F. Sarofim [a], Charles K. Westbrook [b]

[a] Department of Chemical Engineering, The University of Utah, Salt Lake City, UT 84112, USA
[b] Lawrence Livermore National Laboratory, Livermore, CA 94551, USA

Abstract

The relative importance of formation pathways for benzene, an important precursor to soot formation, was determined from the simulation of 22 premixed flames for a wide range of equivalence ratios (1.0–3.06), fuels (C_1–C_{12}), and pressures (20–760 torr). The maximum benzene concentrations in 15 out of these flames were well reproduced within 30% of the experimental data. Fuel structural properties were found to be critical for benzene production. Cyclohexanes and C_3 and C_4 fuels were found to be among the most productive in benzene formation; and long-chain normal paraffins produce the least amount of benzene. Other properties, such as equivalence ratio and combustion temperatures, were also found to be important in determining the amount of benzene produced in flames. Reaction pathways for benzene formation were examined critically in four premixed flames of structurally different fuels of acetylene, *n*-decane, butadiene, and cyclohexane. Reactions involving precursors, such as C_3 and C_4 species, were examined. Combination reactions of C_3 species were identified to be the major benzene formation routes with the exception of the cyclohexane flame, in which benzene is formed exclusively from cascading fuel dehydrogenation via cyclohexene and cyclohexadiene intermediates. Acetylene addition makes a minor contribution to benzene formation, except in the butadiene flame where C_4H_5 radicals are produced directly from the fuel, and in the *n*-decane flame where C_4H_5 radicals are produced from large alkyl radical decomposition and H atom abstraction from the resulting large olefins.
© 2009 The Combustion Institute. Published by Elsevier Inc. All rights reserved.

Keywords: Benzene formation pathways; Benzene formation potential; Structural dependence of benzene chemistry; Premixed flames

1. Introduction

The present study is motivated by the need to develop kinetic mechanisms for hydrocarbons that can simulate the formation of soot in combustion from practical fuels. Practical distillate fuels (aviation and diesel) consist predominantly of *n*-paraffins, iso-paraffins, cyclo-paraffins (naphthenes), and aromatics; gasolines consist also of minor fractions of olefins; and natural gas consists primarily of methane with small amounts of other small paraffins. All of these practical fuels make soot by producing benzene or other small aromatic species, which are the major precursors to soot. Different fuels, with different molecular structures, make benzene in different ways, but once the first small aromatic species are produced, subsequent reaction pathways to soot are

* Corresponding author. Fax: +1 801 585 1456.
E-mail address: westshanghai@yahoo.com (H.R. Zhang).

1540-7489/$ - see front matter © 2009 The Combustion Institute. Published by Elsevier Inc. All rights reserved.
doi:10.1016/j.proci.2008.06.011

expected to be relatively independent of the original fuel.

Consequently, the focus of the present paper is on defining a composite mechanism to include all of the reaction pathways that produce benzene in flames burning a wide range of different fuels. In addition to contributing to particulate pollution via soot generation, combustion-generated benzene has also raised public health concerns since benzene is a carcinogen itself and participates in the formation of higher aromatics, many of which are also known carcinogens.

Benzene formation pathways via addition of C_4 species to acetylene or combination of C_3 species have been studied extensively. Reactions adding C_4 radicals to molecular acetylene were proposed by Westmoreland et al. [1] and Frenklach et al. [2] to be the principal formation pathways for the first aromatic rings via the first class of reactions in the list below.

Class1,	R1 :	$C_2H_2 + CH_2CHCHCH$	=	$C_6H_6 + H$
	R2 :	$C_2H_2 + HCCHCCH$	=	C_6H_5
Class2,	R3 :	$H_2CCCH + H_2CCCH$	=	C_6H_6
	R4 :	$H_2CCCH + CH_2CCH_2$	=	$C_6H_6 + H$
	R5 :	$H_2CCCH + H_2CCCH$	=	$C_6H_5 + H$
	R6 :	$H_2CCCH + CH_2CHCH_2$	=	$FULVENE + 2H$
Class3,	R7 :	$C_5H_5 + CH_3 \rightarrow C_5H_5CH_3$ and radical $\rightarrow C_6H_6$		
Class4,	R8 :	$cycloC_6 - R \rightarrow C - C_6H_{10} \rightarrow C - C_6H_8 \rightarrow C_6H_6$		
Class5,	R9 :	$C_6H_5 - R + H$	=	$C_6H_6 + R$

Reactions of propargyl radicals (Class 2) present an alternative reaction pathway to benzene and phenyl radical [3]. Reactions 3 and 5 of the self-combination of propargyl radicals have been studied in detail [3–7] and is considered by many to provide the dominant route to the first aromatic rings. Other benzene formation pathways have also been proposed, including the combination of CH_3 and C_5H_5 radicals via cyclo-dienes and derivatives R7 [8], the cascading dehydrogenation of cyclohexane derivatives R8 [9,10], and de-alkylation of branched benzenes R9 [11]. The entire subject has been reviewed in detail by Miller et al. [12,13]. The rates of the important reactions in the present benzene formation study are summarized in Table 1.

Earlier modeling studies, however, often suffered from a limited set of available data and usually focused on a single fuel and a single benzene formation pathway, with the exception of studies by Kohse-Hoeinghaus et al. [18–20] and Hoyermann et al. [21], who compared the benzene formation in pairs of flames with C_2–C_5 fuels. In addition, many uncertainties have been associated with reactions that involve aromatic precursor species. A recent accumulation of experimental data on the production of soot precursors for fuels from natural gas to kerosene, together with advances in kinetics of small, unsaturated hydrocarbon species, have created a unique opportunity to investigate major benzene formation pathways in flames based on the chemical structure of the fuel. In the present study, benzene concentration predictions and benzene formation pathway analyses based on the fuel structure, will be reported for 22 premixed flames with 14 different fuels, which include C_1–C_{12} fuels with equivalence ratios

Table 1
Benzene formation reactions used in the present calculation

Reactions	A	n	E	References
1. HACA reactions				
1a. $CH_2CHCHCH + C_2H_2 = C_6H_6 + H$	1.6×10^{16}	−1.33	5400	[14]
1b. $HCCHCCH + C_2H_2 = C_6H_5$	9.6×10^{70}	−17.77	31300	[14]
1c. $CH_2CHCCH_2 + C_2H_2 = C_6H_6 + H$	3×10^{11}	0	14900	[22]
1d. $H_2CCCCH + C_2H_2 = C_6H_5$	3×10^{11}	0	14900	[22]
2. C_3 Combination reactions				
2a. $H_2CCCH + H_2CCCH = C_6H_6$	3×10^{11}	0	0	[15]
2b. $H_2CCCH + CH_2CCH_2 = C_6H_6 + H$	1.4×10^{12}	0	10000	[16]
2c. $H_2CCCH + H_2CCCH = C_6H_5 + H$	1.5×10^{12}	0	3000	[17] × .75
2d. $H_2CCCH + CH_2CHCH_2 = Fulvene + 2H$	1.0×10^{12}	0	3000	[17] × .5
3. $C\text{–}C_5H_5 + CH_3 = methyl\ cyclopentadiene$	1.76×10^{50}	−11.0	18600	[8,22]
4. $C_6H_5CH_3 + H = C_6H_6 + CH_3$	1.20×10^{13}	0	5148	[11]

between 1.0 and 3.06 and pressures between 20 and 760 torr [10,22–39].

2. Precursor chemistry of benzene formation

Benzene can be produced by a variety of kinetic pathways from a number of precursor species. Reliable kinetics for these precursors are required to achieve numerical accuracy in predicting levels of aromatic species in flames; in particular, kinetics for key species and reactions that are chemically related to allyl radical have been overlooked in many mechanisms.

Substantial improvements have been made for olefin chemistry during the development of the present mechanism, the Utah Surrogate Mechanisms, particularly for larger olefins that have significant impacts on predicted benzene concentrations in flames of large *n*-alkanes [40,41].

Reactions of species producing allyl and propargyl radicals, such as allene and propyne, are critical for the correct prediction of benzene concentrations. Reactions involving propyne, however, have been largely overlooked in early mechanism development, and C_3H_4 concentrations measured in experiments using mass spectrometry have often been assigned to the allene isomer. In recent studies, however, the measured peak concentration of propyne was found to be 270 ppm versus 150 ppm for allene in a *n*-heptane flame [37], and more propargyl radicals are formed from propyne via hydrogen abstraction than those obtained from allene [41]. Reactions of propyne have a lower energy barrier than those involving allene since it is easier to abstract hydrogen from an sp^3 carbon than from an sp^2 carbon. Recent flame measurements [36–38] have used gas chromatography to identify structural isomers and to provide added insight on how C_3H_4 isomers are formed and consumed. This experimental data have aided in the generation of the reactions involving propyne in the present mechanism and were essential in predicting the benzene concentrations in flames burning different fuels.

Rates of reactions involving acetylene and vinyl radical are also very important for benzene production because the combination of vinyl and methyl radicals is a major formation route for allyl radical. Both acetylene and vinyl radical are formed from dehydrogenation of ethylene, and the selection of the vinyl decomposition rates and reactions involving C_4 species have also been critically examined [42].

In summary, a group of precursors has been included in the present mechanism, and the species include propylene, 1-butene, 2-butene, isobutylene, propyne, 1-butyne, allene, 1,3-butadiene, vinyl acetylene, and di-acetylene, reactions of which have been critically examined and modified. These reactions are important for the formation of the intermediates for the first aromatic rings.

3. Numerical results

With the above-mentioned improvements in reactions of olefins and allyl-related species, simulation results when burning fuels using the Utah Surrogate Mechanisms have been compared favorably in earlier studies with experimental data of a few atmospheric premixed flames of *n*-heptane ($\phi = 1.0$ and 1.9) [41–44], isooctane ($\phi = 1.9$), *n*-decane ($\phi = 1.7$) [43], gasoline ($\phi = 1.0$) and kerosene ($\phi = 1.7$) [9], and a 30 Torr premixed flame of cyclohexane ($\phi = 1.0$) [45].

In the present study, the mechanism has been used to simulate 22 premixed flames using CHEMKIN IV, with fuels ranging from C_1 to C_{12} species, including paraffins, olefins, acetylenes, aromatics, and liquid fuels. Experimental conditions such as fuel, inert and oxidizer levels, maximum temperatures and other quantities are summarized for these flames in Table 2, together with measured and predicted maximum benzene concentrations and the benzene peak locations for each flame. The simulated and experimental benzene profiles in most of these flames are compared in Fig. 1. The maximum benzene concentrations in 15 out of the 22 flames were predicted within 30% of the experimental data, and the overall agreement between computed and experimental results is very good.

4. Benzene level and fuel structure

The approach of using data from multiple flames for many structurally different fuels, using a single kinetic reaction mechanism, provides an opportunity to cross-examine these benzene formation mechanisms and relate how the benzene reaction pathways depend on the initial fuel structure and experimental conditions.

The flames that produce most benzene include Flame 12 (C_3H_6 $\phi = 2.3$, 1220 ppm), Flame 13 (1,3-C_4H_6 $\phi = 2.4$, 1300 ppm) and Flame 21 (kerosene $\phi = 1.7$, 1090 ppm). The propylene flame produces a factor of two more benzene than that obtained in Flame 11 (C_2H_4 $\phi = 3.06$, 575 ppm) and a factor of five more than that in Flame 10 (C_2H_4 $\phi = 2.76$, 250 ppm), although both ethylene flames have higher equivalence ratios. The propylene flame produces large amounts of C_3 benzene precursors directly from fuel consumption, while the ethylene flame chemistry must follow a much more complex and slower path to produce benzene.

Another example of the importance of the C_3 reaction pathways is the substantially higher benzene concentrations in Flame 3 (C_3H_8 $\phi = 2.78$,

Table 2
Experimental conditions and measured and predicted maximum benzene concentrations in 22 premixed flames

#	Fuel	Inert Ar, %	C/O	Eq. ratio	*P* torr	*T* (Max) K at cm	Flow rate[a]	Exp. Max. $[C_6H_6]$[b] at cm	Cal. Max. $[C_6H_6]$[b] at cm	Deviation%	Ref.
F1	CH_4	0.453	0.626	2.50	760	1605 at 0.4	7.19×10^{-2}	280 at 0.8	141 at 0.8	−49.6	[22]
F2	C_2H_6	0.453	0.715	2.50	760	1600 at 0.24	1.00×10^{-1}	230 at 0.8	205 at 0.8	−10.9	[22]
F3	C_3H_8	0.44	0.833	2.78	760	1640 at 0.4	9.21×10^{-2}	840 at 0.35	922 at 0.32	+9.8	[23]
F4	C_3H_8	0.424	0.54	1.80	30	2190 at 0.95	2.27×10^{-2}	17.5 at 0.75	72.9 at 0.77	+ × 4.2[e]	[24]
F5	C_2H_2	0.05	0.959	2.40	20	1901 at 1.0	1.58×10^{-2}	40 at 0.37	82.7 at 0.37	+ × 2.1[e]	[25]
F6	C_2H_2	0.45	1.00	2.50	19.5	1850 at 1.0	3.46×10^{-2}	58.9 at 0.6	39.1 at 0.64	−33.6	[26]
F7	C_2H_2	0.55	1.103	2.76	90	1988 at 0.73	3.43×10^{-2}	140 at 0.6	96.7 at 0.55	−30.9	[27]
F8	C_2H_4	0.5	0.634	1.90	20	2192 at 1.7	2.37×10^{-2}	33.1 at 0.9	11.4 at 0.77	− × 2.9[e]	[28]
F9	C_2H_4	0	0.80	2.40	760	1815 at 0.1	7.36×10^{-2}	936 at 0.15	136 at 0.14	− × 6.9[e]	[29]
F10	C_2H_4	0.656	0.92	2.76	760	1600 at 0.3	1.12×10^{-1}	250 at 0.35	212 at 0.35	−15.2	[30]
F11	C_2H_4	0.578	1.02	3.06	760	1420 at 0.3	7.21×10^{-2}	575 at 1.0	553 at 1.0	−3.8	[31]
F12	C_3H_6	0.25	0.773	2.32	37.5	2371 at 0.71	3.53×10^{-2}	1220 at 0.39	927 at 0.39	−24.0	[32]
F13	C_4H_6	0.03	0.874	2.40	20	2310 at 1.65	2.08×10^{-2}	1300 at 0.85	1490 at 0.85	+14.6	[33]
F14	C_6H_6	0.3	0.717	1.79	20	1905 at 0.2	2.19×10^{-2}	N/A	N/A	Good	[34]
F15	C_6H_6	0.752[c]	0.72	1.80	760	1850 at 0.45	5.07×10^{-2}	N/A	N/A	Good	[35]
F16	C_7H_{16}	0.841[c]	0.318	1.00	760	1843 at 0.25	2.83×10^{-1}	12 at 0.08	1.77 at 0.09	− × 6.8[e]	[36]
F17	C_7H_{16}	0.73[c]	0.605	1.90	760	1640 at 0.30	6.50×10^{-2}	75 at 0.225	75.8 at 0.23	+1.1	[37]
F18	i-C_8H_{18}	0.682[c]	0.608	1.90	760	1670 at 0.30	5.56×10^{-2}	292 at 0.21	455 at 0.23	+55.8	[37]
F19	$C_{10}H_{22}$	0.682[c]	0.558	1.73	760	1688 at 0.20	6.68×10^{-2}	65 at 0.10	68.5 at 0.10	+5.4	[38]
F20	gasoline	0.768[c], 0.01[d]		0.9-1	760	1990 at 0.046	1.28×10^{-1}	344 at 0.05	330 at 0.05	−4.1	[39]
F21	kerosene	0.684[c]		≈1.7	760	1775 at 0.20	7.96×10^{-2}	1090 at 0.1	850 at 0.75	−22.0	[38]
F22	C–C_6H_{12}	0.325	0.333	1.00	30	1960 at 0.6	2.14×10^{-2}	473 at 0.09	498 at 0.09	+5.3	[10]

[a] g/(cm^2 s).
[b] Measured and predicted benzene concentrations in ppm.
[c] Diluted by inert N_2.
[d] Also using krypton as internal standard.
[e] ×4.2 means a factor of 4.2.

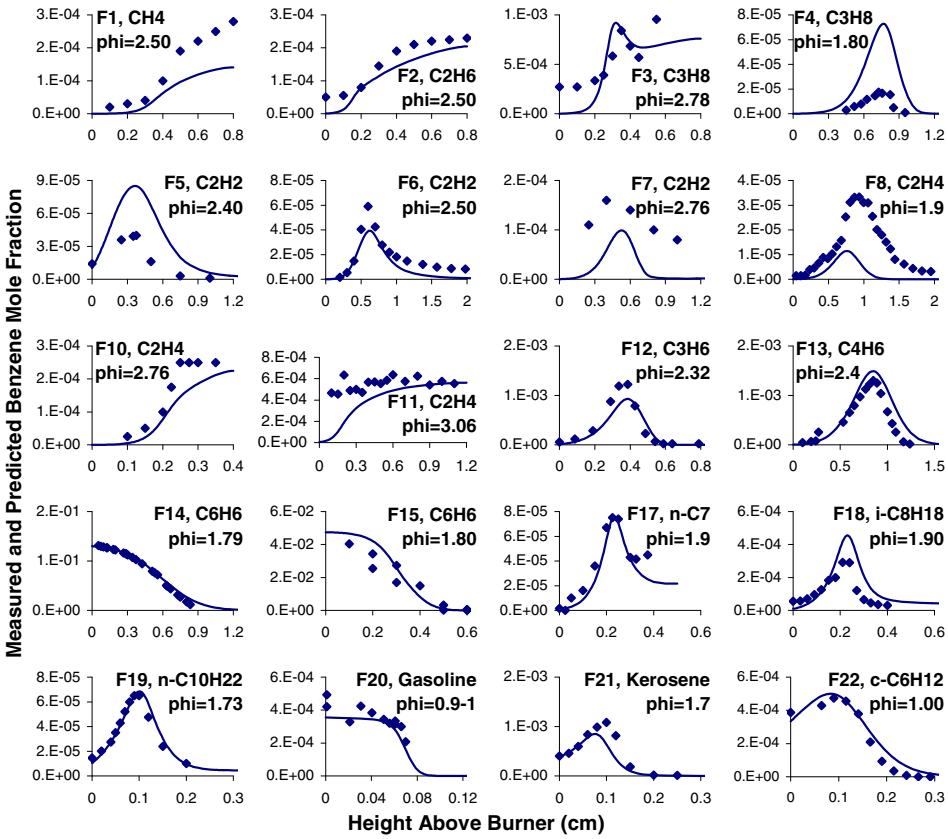

Fig. 1. The predicted and experimental mole fractions of benzene in 20 premixed flames. The symbols represent the experimental data; the lines the simulations.

840 ppm), compared to those obtained in the smaller alkane-fueled Flame 1 (CH_4 $\phi = 2.50$, 280 ppm) and Flame 2 (C_2H_6 $\phi = 2.50$, 230 ppm). Again, the C_3 fuel produces much greater levels of C_3 benzene precursors directly from fuel consumption than the other flames.

The high benzene formation in the 1,3-butadiene flame is a consequence of the direct formation of C_4 precursors from the fuel. Higher C_4 species in the butadiene flame enhance benzene formation via acetylene addition reactions R1 and R2, with the benzene production rates comparable to those from C_3 species combination.

Another structure-dependent example is benzene formation in the kerosene-fueled Flame 21. The kerosene mixture contains 10% methyl cyclohexane [9] in addition to the major fuel component n-$C_{12}H_{26}$ (73.5%), and the methyl cyclohexane produces a significant increase in benzene concentration. The benzene level was reported to be 1090 ppm, as compared to the maximum benzene concentration of 65 ppm in the n-$C_{10}H_{22}$ Flame 19, although both flames had very similar equivalence ratio, inert fraction, cold gas flow rate, and other physical conditions. A similarly very high level of benzene formation was also observed in the cyclohexane Flame 22. The 473 ppm maximum benzene mole fraction measured in this 30 torr stoichiometric flame is 40 times that obtained in the atmospheric pressure, stoichiometric n-heptane Flame 16 (n-C_7H_{16} $\phi = 1.0$, 12 ppm). Benzene formation from the cyclohexane fraction (8.6% by volume) and the de-alkylation of aromatics in the gasoline Flame 20 offsets the consumption rate of the benzene fraction in the fuel, leading to an interesting plateau in the benzene profile (Fig. 1).

Benzene formation also depends strongly on other fuel structural features. For example, Flame 18 (i-C_8H_{18} $\phi = 1.90$, 292 ppm) produces much higher benzene levels than Flame 17 (n-C_7H_{16} $\phi = 1.90$, 75 ppm). Both flames were operated under the almost identical experimental conditions. The much higher benzene concentrations in the isooctane flame reflect the preferred formation of C_3 and C_4 precursors, while the n-heptane flame produces primarily ethylene precursors that yield C_3 species in subsequent steps. For example, the measured mole fractions of propylene in n-heptane and isooctane flames at the benzene peak positions of each flame are 2080:4500 ppm (n-C_7:i-C_8); those of allene 150:1200 ppm; those of

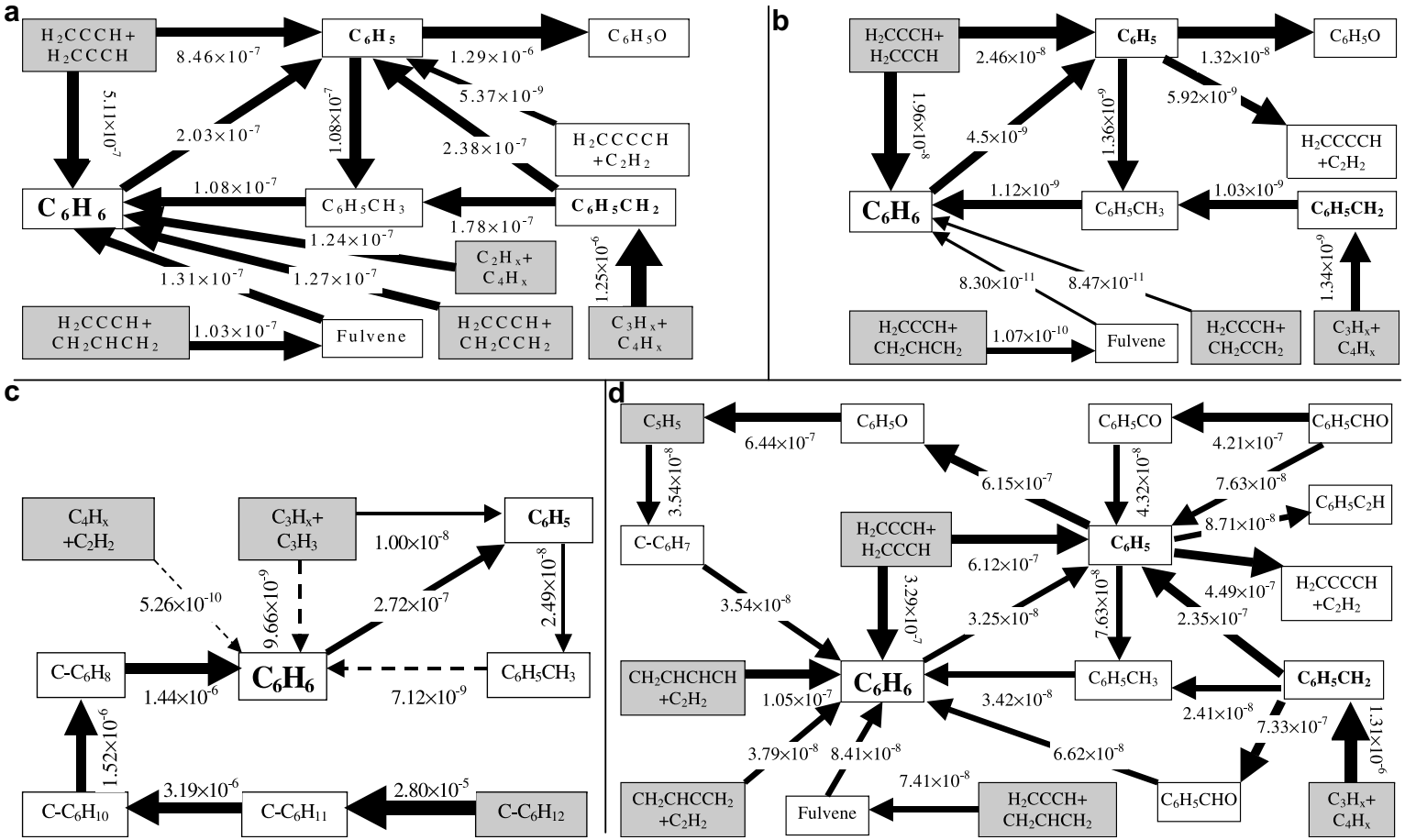

Fig. 2. Major benzene formation pathways in the (a) F19 *n*-decane [38], (b) F6 acetylene [26], (c) F22 cyclohexane [10], (d) F13 1,3-butadiene flames [33]. The shaded areas represent benzene precursors.

ethylene 22,000:9500 ppm. Those values were also well predicted using the mechanism [41–43]. The predicted mole fractions of allyl radical, which was not measured, are 42:103 ppm; those of propargyl radical 129:209 ppm; those of isobutylene 21:4400 ppm; those of isobutylenyl radical 0.7:61 ppm. Studies of these two flames and those that include cyclo-paraffins (Flames 20, 21, and 22) reveal a pattern of benzene formation potential that is related to how the carbon atoms are connected in the fuel molecule. More benzene is formed in flames of cyclo-paraffins than in those of other paraffins. Normal paraffin flames produce the least amount of benzene under similar flame conditions.

In addition to fuel structure, benzene formation depends strongly on the equivalence ratio of the fuel/oxidizer mixture, since oxidation is favored in leaner flames. For example, the measured maximum benzene concentration in Flame 4 (C_3H_8 $\phi = 1.8$, 17.5 ppm) is only 2% of that obtained in the richer Flame 3 (C_3H_8 $\phi = 2.78$, 840 ppm). Of the four ethylene flames, the richest Flame 11 (C_2H_4 $\phi = 3.06$, 575 ppm) produces about 20 times more benzene than the leanest Flame 8 (C_2H_4 $\phi = 1.9$, 33.1 ppm), and the same trend is seen between the stoichiometric and rich *n*-heptane Flames 16 and 17.

5. Detailed benzene production analysis

Four flames will be critically examined in this section, flames which represent different fuel classes of large *n*-paraffins, acetylenes, C_4 dienes, and cyclohexanes. Because of the structural differences in these fuels, the dominant benzene formation pathways are unique in each flame. Benzene formation pathways have been presented in Fig. 2. The rates of important pathways at the location of peak benzene concentration in each flame are shown along the arrow indicating the reaction direction; the thickness of the arrow, representing the relative magnitude of the reaction rate in log scale, is normalized to the highest rate of formation routes in each flame. The shaded areas represent major benzene precursors that include C_2H_2, C_3H_3, C_3H_4, C_3H_5, C_4H_3, C_4H_5, C_5H_5, C–C_6H_7 and C–C_6H_8.

In the *n*-decane flame, benzene formation is dominated by C_3 species combination. The C_3H_3 radical combination (R3) accounts for 51% of the total benzene formation, followed by contributions of 13% from the combination of C_3H_3 and C_3H_5 radicals via the intermediate fulvene (R6), 13% from the combination of C_3H_4 and C_3H_3 radical (R4), 12% from acetylene addition (R1 and R2), and 11% from the de-alkylation of toluene (R9, –CH_3). The contribution from the self-combination of C_3H_3 radicals via phenyl radical (R5) is more difficult to assess because the importance of phenyl hydrogenation ($C_6H_5 \rightarrow C_6H_6$) is displaced by that of the reverse hydrogen abstraction of benzene. It is noteworthy, however, that reaction R5 is 66% faster than the fastest direct formation (R3) producing benzene.

The detailed *n*-decane reaction mechanism shows that H atom abstraction from the fuel, followed by β-scission of resulting decyl radicals, produce large amounts of C_3–C_8 olefins [41–43]. These olefins then decompose to produce the high levels of C_3 and C_4 precursors to benzene formation. For example, $CH_2CHCHCH$ comes from hydrogen abstraction from 1,3-butadiene and C_3H_3 is formed mainly from CH_2CHCCH_2 radical decomposition (R10, the reverse reaction dominates) and hydrogen abstraction from C_3H_4 isomers (R11 and R12).

$$\text{R10: } H_2CCCH + CH_3 = CH_2CHCCH_2 + H \quad (43\%)$$
$$\text{R11: } CH_3CCH + H = H_2CCCH + H_2 \quad (29\%)$$
$$\text{R12: } CH_2CCH_2 + H = H_2CCCH + H_2 \quad (13\%)$$

In the acetylene flame, the combination of C_3H_3 radicals (R3) is the only significant pathway, which accounts for 94% of benzene formation. All other important routes identified in the *n*-decane flame are insignificant in the acetylene flame. The self-combination of C_3H_3 radicals forming phenyl radical (R5) is 26% faster than the fastest (R3) of the direct benzene formation routes. The crucial precursor C_3H_3 comes from the combination of C_2H_2 and CH_2 (both singlet and triplet) in contrast to its formation from large species (R10–R12) in the *n*-decane flame.

$$\text{R13: } {}^1CH_2 + C_2H_2 = H_2CCCH + H \quad (87\%)$$
$$\text{R14: } {}^3CH_2 + C_2H_2 = H_2CCCH + H \quad (11\%)$$

The cyclohexane flame also includes a single benzene formation pathway that is significantly greater than all other routes. Benzene is produced via the sequential dehydrogenation of the fuel through cyclohexene and cyclohexadiene, and this dominant pathway is two orders of magnitude faster than C_3 species combination and three orders faster than acetylene addition.

The 1,3-butadiene flame provides the most complicated benzene formation mechanism of these four flames, involving significant contributions from both C_3 combination and acetylene addition. The combination of C_3H_3 radicals (R3) accounts for 48% of the total benzene formation, followed by 20% from acetylene addition (R1), 12% from the combination of C_3H_3 and C_3H_5 radicals via the intermediate of fulvene (R6), 10% from the de-acylation of C_6H_5CHO, 5% from the de-methylation of $C_6H_5CH_3$ (R9), and 5% from the combination of CH_3 and C_5H_5 radicals followed by dehydrogenation (R8). The C_3H_3 radical combination producing phenyl radical (R5) is 86% faster than the fastest (R3) of the

direct formation routes. The unique structure of the butadiene fuel leads to preferential formation of C_4H_5 isomers that produces the significant contribution of acetylene addition. The formation of C_4H_5 isomers also determines the dominance of reaction R10 in the C_3H_3 radical formation (86%), compared to the 8% contribution from the combination of singlet methylene radical and acetylene (R13).

6. Conclusions

The relative importance of pathways to benzene formation has been examined in 22 premixed flames, using a single kinetic reaction mechanism that includes all of the reaction pathways currently understood to lead to benzene formation. The predicted maximum benzene concentrations agree very well overall with the experimental data. Fuel structural properties were found to be critical in determining rates of benzene production via the multiple formation pathways among different fuels in premixed flames. Depending on the fuel structure, different reaction pathways are responsible for benzene production. The present mechanism represents an important step towards providing a unified kinetic description of soot formation in many different fuel mixtures and combustion environments.

Acknowledgment

This research was funded by the University of Utah (C-SAFE), through a contract with the Department of Energy, Lawrence Livermore National Laboratory (B341493).

Appendix A. Supplementary data

Supplementary data associated with this article can be found, in the online version, at doi:10.1016/j.proci.2008.06.011.

References

[1] P.R. Westmoreland, A.M. Dean, J.B. Howard, J.P. Longwell, *J. Phys. Chem.* 93 (25) (1989) 8171–8180.
[2] M. Frenklach, D.W. Clary, W.C. Gardiner Jr., S.E. Stein, *Proc. Combust. Inst.* 20 (1985) 887–901.
[3] H. Hopf, *Chem. Ber.* 104 (5) (1971) 1499–1506.
[4] U. Alkemade, K.H. Homann, *Zeitschrift fuer Physikalische Chemie (Muenchen, Germany)* 161 (1–2) (1989) 19–34.
[5] S.E. Stein, J.A. Walker, M.M. Suryan, A. Fahr, *Proc. Combust. Inst.* 23 (1990) 85–90.
[6] R.D. Kern, K. Xie, *Progress Energy Combust. Sci.* 17 (3) (1991) 191–210.
[7] J.A. Miller, C.F. Melius, *Combust. Flame* 91 (1) (1992) 21–39.
[8] E.R. Ritter, J.W. Bozzelli, A.M. Dean, *J. Phys. Chem.* 94 (6) (1990) 2493–2504.
[9] H.R. Zhang, E.G. Eddings, A.F. Sarofim, *Proc. Combust. Inst.* 31 (2007) 401–409.
[10] M.E. Law, P.R. Westmoreland, T.A. Cool, J. Wang, N. Hansen, T. Kasper, *Proc. Combust. Institut.* 31 (2007) 565.
[11] J. Emdee, K. Brezinsky, I. Glassman, *J. Phys. Chem.* 96 (1992) 2151.
[12] J.A. Miller, M.J. Pilling, J. Troe, *Proc. Combust. Inst.* 30 (2005) 43–88.
[13] J.A. Miller, S.J. Klippenstein, *J. Phys. Chem. A* 107 (39) (2003) 7783–7799.
[14] H. Wang, M. Frenklach, *J. Phys. Chem.* 98 (44) (1994) 11465–11489.
[15] C.H. Wu, R.D. Kern, *J. Phys. Chem.* 91 (1987) 6291.
[16] Y. Hidaka, T. Nakamura, A. Miyauchi, T. Shiraishi, H. Kawano, *Int. J. Chem. Kinet.* 21 (1989) 643–666.
[17] A. Burcat, M. Dvinyaninov, *Int. J. Chem. Kinet.* 29 (1997) 505–514.
[18] M. Kamphus, M. Braun-Unkhoff, K. Kohse-Hoeinghaus, *Combust. Flame* 152 (1/2) (2008) 28–59.
[19] B. Atakan, A. Lamprecht, K. Kohse-Hoinghaus, *Combust. Flame* 133 (4) (2003) 431–440.
[20] A. Lamprecht, B. Atakan, K. Kohse-Hoinghaus, *Proc. Combust. Inst.* 28 (2000) 1817–1824.
[21] K. Hoyermann, F. Mauss, T. Zeuch, *Phys. Chem. Chem. Phys.* 6 (14) (2004) 3824–3835.
[22] N.M. Marinov, W.J. Pitz, C.K. Westbrook, M.J. Castaldi, S.M. Senkan, *Combust. Sci. Technol.* 116–117 (1–6) (1996) 211–287.
[23] N.M. Marinov, M.J. Castaldi, C.F. Melius, W. Tsang, *Combust. Sci. Technol.* 128 (1–6) (1997) 295–342.
[24] T.A. Cool, K. Nakajima, C.A. Taatjes, et al., *Proc. Combust. Inst.* 30 (2005) 1681.
[25] P.R. Westmoreland, J.B. Howard, J.P. Longwell, *Proc. Combust. Inst.* 21 (1988) 773–782.
[26] E. Bastin, R.M. Delfau, M. Reuillon, C. Vovelle, J. Warnatz, *Proc. Combust. Inst.* 22 (1988) 313–322.
[27] H. Bockhorn, F. Fetting, H.W. Wenz, *Berichte der Bunsen-Gesellschaft* 87 (11) (1983) 1067–1073.
[28] A. Bhargava, P.R. Westmoreland, *Combust. Flame* 113 (3) (1998) 333–347.
[29] A. Ciajolo, A. D'anna, R. Barbella, A. Tregrossi, A. Violi, *Proc. Combust. Inst.* 26 (1996) 2327–2333.
[30] S.J. Harris, A.M. Weiner, *Combust. Sci. Technol.* 31 (3–4) (1983) 155–167.
[31] M.J. Castaldi, N.M. Marinov, C.F. Melius, et al., *Proc. Combust. Inst.* 26 (1996) 693–702.
[32] B. Atakan, A.T. Hartlieb, J. Brand, K. Kohse-Hoinghaus, *Proc. Combust. Inst.* 27 (1998) 435–444.
[33] J.A. Cole, J.D. Bittner, J.P. Longwell, J.B. Howard, *Combust. Flame* 56 (1) (1984) 51–70.
[34] J.D. Bittner, J.B. Howard, *Proc. Combust. Inst.* 18 (1980) 1105–1116.
[35] A. Tregrossi, A. Ciajolo, R. Barbella, *Combust. Flame* 117 (3) (1999) 553–561.
[36] C. Vovelle, Personal Communication, 2002.
[37] A. El Bakali, J.L. Delfau, C. Vovelle, *Combust. Sci. Technol.* 140 (1–6) (1998) 69–91.
[38] C. Doute, J.L. Delfau, R. Akrich, C. Vovelle, *Combust. Sci. Technol.* 106 (4–6) (1995) 327–344.

[39] A. Hakansson, K. Stromberg, J. Pedersen, J.O. Olsson, *Chemosphere* 44 (5) (2001) 1243–1252.
[40] H.R. Zhang, E.G. Eddings, A.F. Sarofim, *Energy Fuels* 21 (2) (2007) 677–685.
[41] H.R. Zhang, E.G. Eddings, A.F. Sarofim, *Energy Fuels* 22 (2) (2008) 945–953.
[42] H. Zhang, Numerical Combustion of Commercial Fuels and Soot Formation, Ph.D. dissertation, Department of Chemical Engineering, University of Utah (2005).
[43] H.R. Zhang, E.G. Eddings, A.F. Sarofim, *Combust. Sci. Technol.* 179 (1–2) (2007) 61–89.
[44] H.R. Zhang, E.G. Eddings, A.F. Sarofim, C.K. Westbrook, *Energy Fuels* 21 (4) (2007) 1967–1976.
[45] H.R. Zhang, L.K. Huynh, N. Kungwan, Z. Yang, S. Zhang, *J. Phys. Chem. A* 111 (2007) 4102–4115.